Bull. Korean Chem. Soc., Vol. 11, No. 6, 1990 487

# Articles

## Potential Profiles and Capacitances of an Ideally Polarizable Electrode/Hard Sphere Electrolyte System

**Sang Youl Kim**

*Department of Physics, Ajou University, Suwon 441-749*

**K. Vedam**

*Materials Research Laboratory The Pennsylvania State University University Park, Pennsylvania 16802.*

*Received June 28, 1990*

A complete potential profile of an electrical double layer is calculated from a distribution function of charged particles based upon a model where the effect of a charged electrode and the finite size of ion are explicitly included. Electrons which are distributed on the electrode surface are assumed not to penetrate the electrode/electrolyte boundary. Formation of the constant density regions and their effects on potential and the electrical double layer capacitances are studied in great detail. The distribution of surface electrons as well as the constant density regions are found to be essential in characterizing the electrical double layer. The introduction of the ion size into the prior electrical double layer model of an ideally polarizable electrode/point charged electrolyte system, shows a great improvement in its characteristics mostly at negative potential region.

### Introduction

Compared to the experimental investigations and interests regarding the electrical double layer (EDL) since the early work of Gouy, Chapman and Stern (GCS),[1] theoretical improvement of the GCS theory is still in its primitive stage. Effects of the charged electrode on the reflectance spectra have been studied under jellium models for the ideally polarizable electrode (IPE).[2] The importance of electron contribution is emphasized via electrionic capacitor model over that of the molecular capacitor model.[3] Electron-density functions of metal/vacuum interface sometimes were used for metal/electrolyte interface study despite their non-correspondency.[4] Considering a strong screening of the electrolyte, a model based on impentrable electrons of metal electrode has been also introduced.[5] However, the latter model neglects the finite size of ions, whereas all the earlier studies had overemphasized the effect of metal electrode by applying the electron density function of metal/vacuum interface into metal/electrolyte interface study without modification. In the present article, the prior model of EDL which was composed of a simplified jellium for IPE and point charged ions for electrolyte is revised in such a way that it represents a more realistic model. Since the model of the simplified jellium for IPE is believed to represent the electrode side of the EDL better than the electrolyte side of it, most improvements made in the present article are about the electrolyte side. These improvements are along the line of taking the ion size into consideration by introducing layers of constant charge density between IPE and the electrical diffuse layer.

For the layers of constant charge density, there can be two such layers, depending on the electrode polarity, the magnitude of the potential difference between the electrode and bulk electrolyte, and the size of the counterion. The first layer is that of zero charge density region, whose thickness is the same as the radius of the counterion. This layer is due to the limit of the counterion in accessing the surface of a metal electrode, in other words, the center of the counterion can not approach the surface of the electrode closer than its radius. This layer represents Stern layer, and the thickness of this layer is determined by the size of the counterion. When the counterion hydrates, hydration effect is taken into account through the use of the hydrated radius of the counterion. The existence of the second layer of constant change density can be recognized if one considers the closest packing density of the counterion. The concept of a closest packing density of atoms is quite well established in the solid state physics[6] and it is quite reasonable to accept that a density of a material can hardly exceed that of the closest packing density. Thus it is not too artificial to impose a limit such that the concentration of a counterion should not exceed this closest packing density. This closest packing density, or a saturation density, is directly calculable from the size of the counterion and vice versa. Thickness of this layer, which might be called as the saturation thickness, depends on the potential difference between IPE and bulk liquid as well as the size of the counterion. This saturation layer may not exist at smaller potential for larger counterions. In the present article, based on an EDL model with hard sphered electrolyte, complete potentials profiles throughout the EDL region are obtained and the EDL characteristics are investigated. It is also demonstrated that the layers of constant charge density together with the charged electrode play a very important role in the study of the EDL characteristics.

### Theory

The concentration profile of a counterion as a functions of a distance $x$ measured from a semi-infinite planar electrode

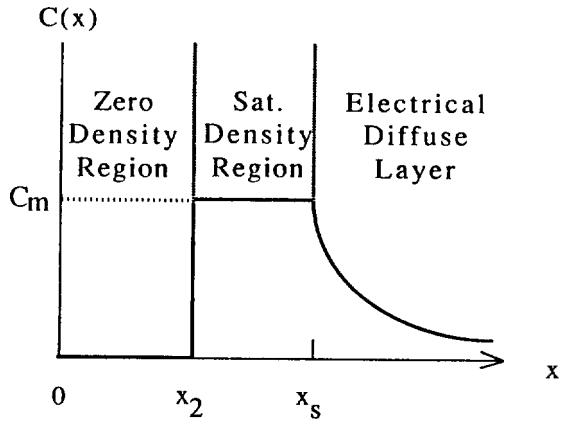


**Figure 1.** Schematic diagram of concentration profile of counterion in the vicinity of electrode. Two constant density layers are labelled as I) and II) for the zero density layer and for the saturation density layer, respectively.

is schematically presented in Figure 1. Two constant density regions, that is the zero density layer which represents the Stern layer and the saturation density layer where the saturation concentration of the counterion is denoted as $C_m$, are located between the electrode and the electrical diffuse layer. For the evaluation of potential profile, potential function $\phi$ as a function of distance $x$ measured from the electrode/electrolyte interface, is suggested as shown below.

$$\frac{d[\phi(x)-\phi_m]}{dx} = -sgn(\phi_m)(2N_0kT/K_m\varepsilon_0)^{1/2} [e^{\beta|\phi(x)-\phi_m|}-1-\beta[\phi(x)-\phi_m]]^{1/2} \quad x\leqq 0 \quad (1)$$

$$\phi(x) = ax+b \quad 0\leqq x\leqq x_2 \quad (2)$$

$$\phi(x) = sgn(\phi_m)eC_mZx^2/2\varepsilon + hx+g \quad x_2\leqq x\leqq x_s \quad (3)$$

$$\phi(x) = (4/Z\beta)\tanh^{-1}[\tanh\{Z\beta\phi(x_s)/4\}e^{-\kappa(x-x_s)}] \quad x_s\leqq x \quad (4)$$

where $\phi_m$ is the potential applied on the electrode with respect to bulk electrolyte, sgn($\phi_m$) is the sign of $\phi_m$, $N_0$ is the bulk electron density of the electrode, $k$ is the Boltzmann constant, $T$ is temperature, $C_m$ is the saturation concentration of the counterion, $Z=|Z_i|$, $Z_i$ is the charge of the species $i$ ($Z-Z$ type electrolyte), $x_s$ is a saturation coordinate such that when $x_s>x_2$, then $x_s-x_2$ means the saturation thickness, $\beta=e/kT$, $\kappa=|Ze|(2C_0/\varepsilon kT)^{1/2}$, which is identified as the reciprocal Debye-Hueckel length, $C_0$ is the bulk concentration of electrolyte, $\varepsilon$, $\varepsilon_0$ are the permittivities of solvent and vacuum respectively, and $K_m$ is the effective dielectric constant of the metal electrode at the surface region where the electron density differs from the bulk density. Stern thickness, or $x_2$ which is identified as the radius of the counterion, is approximately related to the saturation concentration $C_m$ as

$$N_AC_m = (1/2\ x_2)^3 \quad (5a)$$

where $N_A$ is the Avogadro Number, $C_m$ is in mol/cm$^3$ and $x_2$ is in centimeters. Eq. (5a) can be rewritten in a conventional unit as

$$x_2 = 5(0.6023C_m)^{-1/3} \quad (5b)$$

where $C_m$ is in mol/liter and $x_2$ is in angstroms.

For a complete potential profile from the electrode to bulk electrolyte, five unknown variables $a$, $b$, $h$, $g$, and $x_s$ should be determined from appropriate boundary conditions. Once the potential profile is determined, other quantities like the concentration profile of ions in electrolyte or the electron distribution function at the electrode surface can be obtained form the corresponding equations of Eqs. (6) and (7). Let $C_i(x)$ be the concentration function of the species $i$ in electrolyte near the interface and $N(x)$ be the function of the electron volume density near the electrode surface, then assuming Boltzmann distribution, it can be shown that

$$C_i(x) = C_0e^{-Z_i\beta\phi(x)} \quad x\geqq x_s \quad (6)$$

$$N(x) = N_0e^{\beta[\phi(x)-\phi_m]}. \quad x\leqq 0 \quad (7)$$

There can be three boundaries, namely at $x=0$, $x=x_2$, and $x=x_s$. At each boundary, the boundary conditions are as follow.

*At* $x=0$,

$$\phi(0) = b \quad (8a)$$

$$\varepsilon a = -sgn(\phi_m)(2K_m\varepsilon_0kTN_0)^{1/2}\{e^{\beta[\phi(0)-\phi_m]}-1-\beta[\phi(0)-\phi_m]\}^{1/2}. \quad (8b)$$

*At* $x=x_2$,

$$ax_2+b = sgn(\phi_m)eC_mZx_2^2/2\varepsilon + hx_2+g \quad (9a)$$

$$a = sgn(\phi_m)eC_mZx_2/\varepsilon + h. \quad (9b)$$

And at $x=x_s$,

$$\phi(x_s) = sgn(\phi_m)eC_mZx_s^2/2\varepsilon + hx_s+g \quad (10a)$$

$$sgn(\phi_m)eC_mZx_s/\varepsilon + h = -(8kTC_0/\varepsilon)^{1/2}\sinh\{Z\beta\phi(x_s)/2\}. \quad (10b)$$

Eqs. (8a), (9a) and (10a) are derived from the condition of potential continuity at $x=0$, $x=x_2$ and $x=x_s$ respectively. Eqs (9b) and (10b) are from the continuity condition of the potential derivative at $x=x_2$ and $x=x_s$. Eq. (8b) can be verified as the charge neutrality condition.[5] This equation is identical to the equation which can be derived by matching the surface charge density of the electrode to the electric field just outside of it through Gauss theorem.[7,8] The potential at $x_s$ can be calculated from the electrical diffuse layer theory[7] with the condition that density of the counterion reaches the saturation density $C_m$ at $x=x_s$. Explicitly, from Eq. (6), equating $C_i(x)$ to $C_m$, $Z_i$ to $Zsgn(\phi_m)$, and $x$ to $x_s$, one can obtain

$$\phi(x_s) = (1/Z\beta)sgn(\phi_m)\ln(C_m/C_0). \quad (11)$$

Now, the five unknown variables $a$,$b$,$h$,$g$, and $x_s$ will be determined from Eqs. (8b) to (10b) with the help of Eqs. (8a) and (11). First, from Eqs. (9b) and (10b), $h$ can be deleted.

$$a+(8kTC_0/\varepsilon)^{1/2}\sinh\{Z\beta\phi(x_s)/2\}= sgn(\phi_m)\,eC_mZ(x_2-x_s)/\varepsilon \quad (12)$$

Hence

$$x_s=x_2-[\varepsilon\, sgn(\phi_m)/eC_mZ]\,[a+(8kTC_0/\varepsilon)^{1/2}\sinh\{Z\beta\phi(x_s)/2\}]. \quad (13)$$

From Eq.(9b) $h$ can be expressed in terms of $a$.

$$h=a-sgn(\phi_m)\,eC_mZx_2/\varepsilon \quad (14)$$

Now, $h$ (Eq.(14)) and $x_s$ (Eq.(13)) are inputted into Eq. (10a) and an expression of $g$ is obtained.

$$g=\phi(x_s)+sgn(\phi_m)\,eC_mZx_2^2/2\varepsilon-ax_2+sgn(\phi_m)\,\varepsilon a^2/(2eC_mZ)-4C_0\,sgn(\phi_m)/(C_mZ\beta)\sinh^2\{Z\beta\phi(x_s)/2\} \quad (15)$$

These expressions of $h$ and $g$ are inserted into Eq. (9a), and after a few steps of calculations, a relation between $a$ and $b$ is obtained as,

$$b=\varepsilon\, sgn(\phi_m)\,a^2/(2eC_mZ)-ax_2+\phi(x_s)-4C_0sgn(\phi_m)/(C_mZ\beta)\sinh^2\{Z\beta\phi(x_s)/2\}. \quad (16)$$

The other relation between $a$ and $b$ can be derived from Eqs. (8a) and (8b).

$$\varepsilon a=-sgn(\phi_m)\,(2K_m\varepsilon_0N_0kT)^{1/2}[e^{\beta(b-\phi_m)}-1-\beta(b-\phi_m)]^{1/2} \quad (17)$$

Finally Eqs. (16) and (17) are numerically solved for $a$ and $b$, and once the values of $a$ and $b$ are obtained, $x_s$, $h$ and $g$ are calculated directly from Eqs. (13), (14) and (15), respectively.

**Special Case.** When the potential difference between the electrode and bulk electrolyte is small and the size of the counterion is large, $x_s$, the calculated saturation cordinate might have smaller value than $x_2$. In such a case, $x_s-x_2$ is negative and it would be meaningless to introduce such a saturated layer of negative thickness. Potential functions when there is no saturated layer are

$$\frac{d[\phi(x)-\phi_m]}{dx}=-sgn(\phi_m)\,(2N_0kT/K_m\varepsilon_0)^{1/2}[e^{\beta|\phi(x)-\phi_m|}-1-\beta[\phi(x)-\phi_m]]^{1/2} \qquad x\leqq 0 \quad (1')$$

$$\phi(x)=ax+b \qquad 0\leqq x\leqq x_2 \quad (2')$$

$$\phi(x)=(4/Z\beta)\tanh^{-1}[\tanh\{Z\beta\phi(x_2)/4\}\,e^{-\chi(x-x_2)}], \qquad x_2\leqq x \quad (18)$$

And the boundary conditions at $x=0$ and $x=x_2$ are

$$\phi(0)=b \quad (8a')$$

$$\varepsilon a=-sgn(\phi_m)\,(2K_m\varepsilon_0kTN_0)^{1/2}[e^{\beta|\phi(0)-\phi_m|}-1-\beta[\phi(0)-\phi_m]]^{1/2} \quad (8b')$$

$$ax_2+b=\phi(x_2) \quad (19)$$

$$a=-(8kTC_0/\varepsilon)^{1/2}\sinh\{Z\beta\phi(x_2)/2\} \quad (20)$$

where $a$, $b$, and $\phi(x_2)$ are unknowns which can be determined from Eqs. (8b'), (19) and (20). Explicitly, from Eqs. (19) and (20)

$$b=\phi(x_2)+x_2(8kTC_0/\varepsilon)^{1/2}\sinh\{Z\beta\phi(x_2)/2\}. \quad (21)$$

Also from Eqs. (8b') and (20) with the help of Eq. (8a')

$$\sinh\{Z\beta\phi(x_2)/2\}=sgn(\phi_m)\,(K_m\varepsilon_0N_0/4\varepsilon C_0)^{1/2}[e^{\beta(b-\phi_m)}-1-\beta(b-\phi_m)]^{1/2}. \quad (22)$$

The $h$ or equivalently $\phi(0)$, and $\phi(x_2)$ are numerically determined from Eqs. (21) and (22).

When the potential $\phi(0)$ is given, the surface charge density of the electrode, which is calculated by integrating the excess (or reduced) volume density of electrons in Eq. (7), is uniquely determined. Capacitances are defined as charge devided by potential. The potential profile inside electrode is closely related to the surface charge density of the electrode and it directly affects the overall EDL potential profile. Also a formation of constant density regions in the electrolye side of the EDL introduces an additional potential profile. These should be properly incorporated in the study of the EDL capacitances and other related characteristics. In the following discussion it is well demonstrated that capacitance, as an example of the EDL characteristics, depends quite sensitively on the applied potential due to the consequently altered potential profile inside the electrode and the constant density regions in electrolyte.

## Results and Discussion

For the electron density $N_0$ of a metal electrode, that of the single crystal gold ($5.9\times10^{22}$/cm$^3$) is used.[6] Bulk concentration, $C_0$, of a potassium chloride solution, which simulates electrolyte, is varied from 0.1 M to 0.0001 M in a uniform logarithmic scale. For te size of $K^+$ ion and that of $Cl^-$ ion, approximate effective ionic radii in an aqueous solution are used. The reported radii are 3.0Å for both ions.[9] The dielectric constant of the electrolyte is assumed to be the same as that of the pure water ($80\epsilon_0$) throughout the constant density regions and the electrical diffuse layer. $K_m$ is approximated to 1, The specific adsorption, which can be defined either as a depletion of the solvation sheath at least partially in the direction of the electrode[10,11] or excess adsorption of ions more than expected from simple coulometric considerations at charged electrode,[12] is not taken into account. Thus the same EDL circumstance as that in our previous model of IPE in an electrical diffuse layer, is simulated by using the same input parameters.[5]

Since effects of the ion size on the EDL characteristics are the primary concern of the present article, results are presented in the same order as those in our earlier publication which dealt with IPE and point charged electrolyte, for a closer comparison. These are; i) potential profiles inside the electrode (Figure 2), ii) absolute potentials at $x=0$ and relative potential drops inside the electrode (Figure 3 and 4,

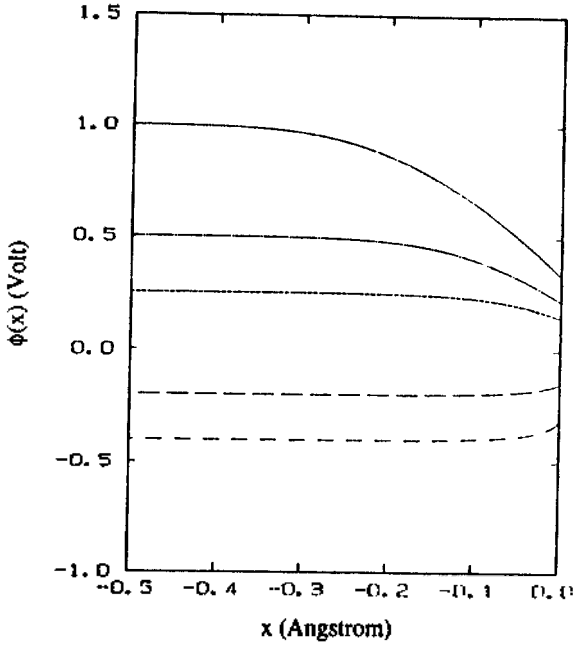


**Figure 2.** Calculated potential profiles inside the electrode (gold) in 0.1 M potassium chloride solution as a function of distance $x$ for the potential differences of 1.0 V (solid line), 0.5 V (—·—), 0.25 V (——), −0.2 V (– – –) and −0.4 V (-----), respectively.

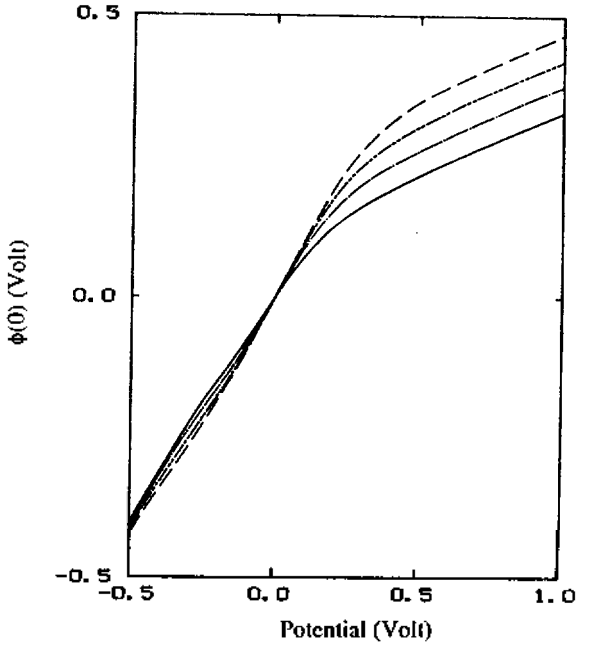


**Figure 3.** The calculated potential at the electrode/electrolyte interface ($x=0$) as a function of potential difference between electrode and bulk electrolyte for bulk concentrations of 0.1 M (solid line), 0.01 M (—·—), 0.001 M (——), and 0.0001 M (– – –) of potassium chloride solution.

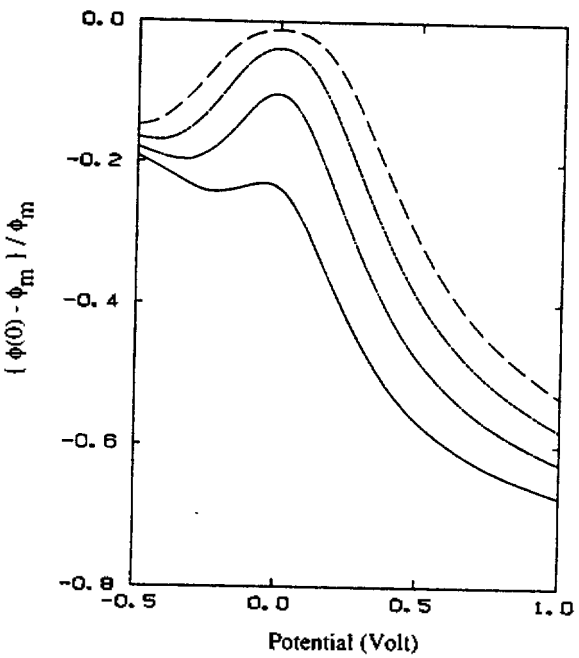


**Figure 4.** The calculated relative potential drop $[\phi_m - \phi(0)]/\phi_m$ at the electrode/electrolyte interface ($x=0$) as a function of potential difference between electrode and electrolyte for bulk concentrations of 0.1 M (solid line), 0.01 M (—·—), 0.001 M (——), and 0.0001 M(– – –) of potassium chloride solution.

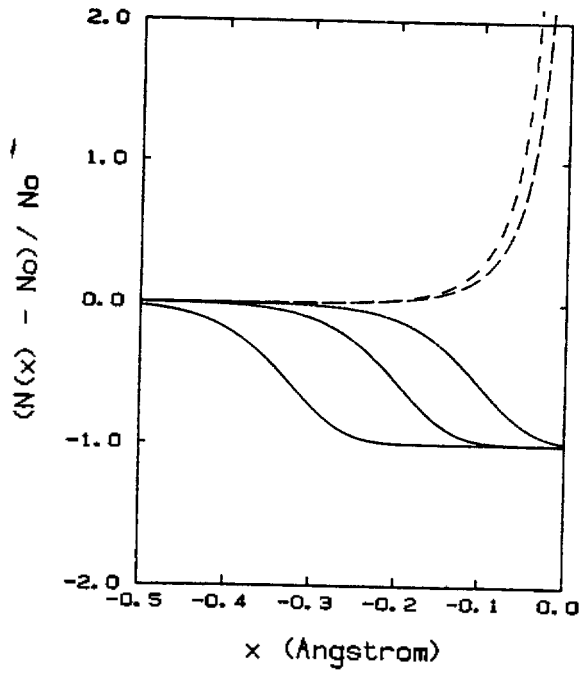


**Figure 5.** The calculated relative electron volume density as a function of distance from the electrode surface for a few selected potential difference of 1.0 V (solid line), 0.5 V (—·—), 0.25 V (——), 0.2V (– – –) and −0.4 V (-----), between electrode and bulk electrolyte. Electrons are accumulated at positive potential and are depleted at negative potential.

respectively), iii) the electron density profiles at the electrode surface (Figure 5), iv) the surface charge density of the electrode (Figure 6), v) potential profiles in the Stern layer, in the saturated concentration layer, and in the electrical diffuse layer (Figure 7), and vi) the calculated EDL capacitances (Figure 8). In addition to the aboves, vii) concentration profiles of cation ($K^+$) and anion ($Cl^-$) (Figure 9 and 10 respectively), viii) dependencies of the saturation coordinate $x_s$ as a function of potential for a few selected electrolyte concentra-

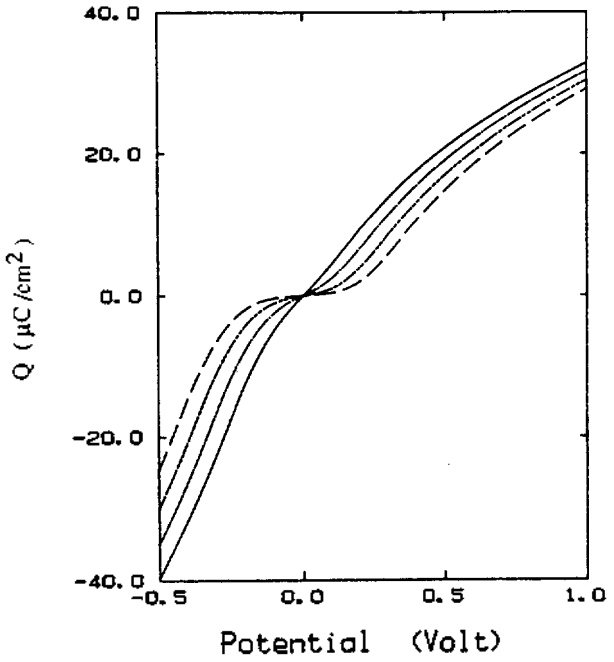


**Figure 6.** The calculated surface charge density of the electrode vs the potential difference between electrode and electrolyte for bulk concentrations of 0.1 M (solid line), 0.01 M (— — —), 0.001 M (— · —), and 0.0001 M (----) of potassium chloride solution.

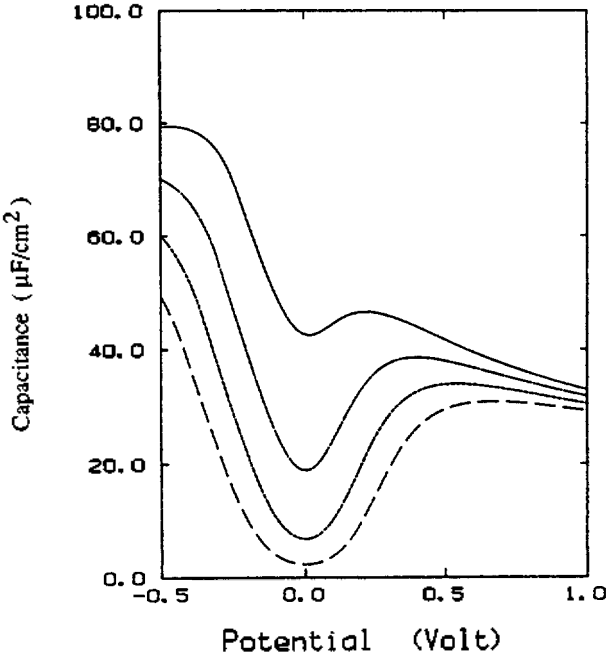


**Figure 8.** The calculated EDL capacitance composed of a gold electrode in 0.1 M (solid line), 0.01 M (— — —), 0.001 M (— · —) and 0.0001 M (----) potassium chloride solution as a function of potential difference between electrode and bulke electrolyte.

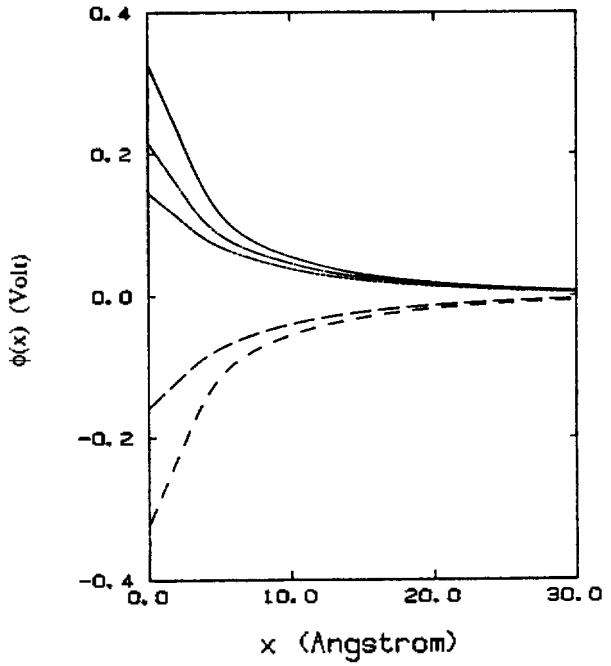


**Figure 7.** The calculated potential profiles near the EDL regions of electrolyte side for potential differences of 1.0 V (solid line), 0.5 V (— — —), 0.25 V (— · —), −0.2 V (— — —) and −0.4 V (----), between electrode and bulk electrolyte.

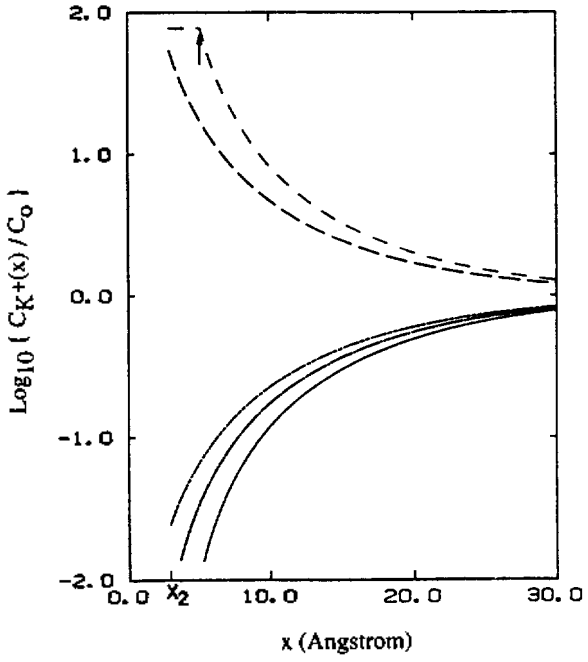


**Figure 9.** The calculated concentration profiles of cation ($K^+$ ion) for potential differences of 1.0 V (solid line), 0.5 V (— — —), 0.25 V (— · —), −0.2 V (— — —) and −0.4 V (----). ($C_o$ = 0.1 M). The saturation coordinate $x_s$ is marked with arrow.

tions (Figure 11), and ix) EDL capacitances at zero potential as a function of electrolyte bulk concentration in a log-log scale (Figure 12) are also presented.

Results are devided into two groups. The first group includes those from Figure 1 to 8, which are in a good qualitative agreement with the earlier results and the second group in Figure 9 through Figure 12, which show the effects of the ion size of the EDL characteristics. For the first group, since a detailed description of similar results appears elsewhere,[5] only a brief summary will follow.

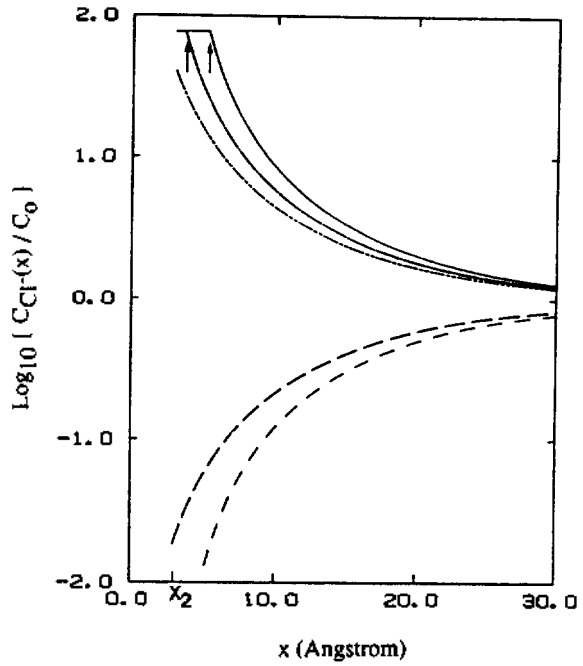


**Figure 10.** The calculated concentration profiles of anion ($Cl^-$ ion) for potential differences of 1.0 V (solid line), 0.5 V(—·—), 0.25V(—··—), −0.2 V(– – –) and −0.4 V (····). ($C_0$ = 0.1 M). The saturation coordinate $x_s$ are marked with arrows.

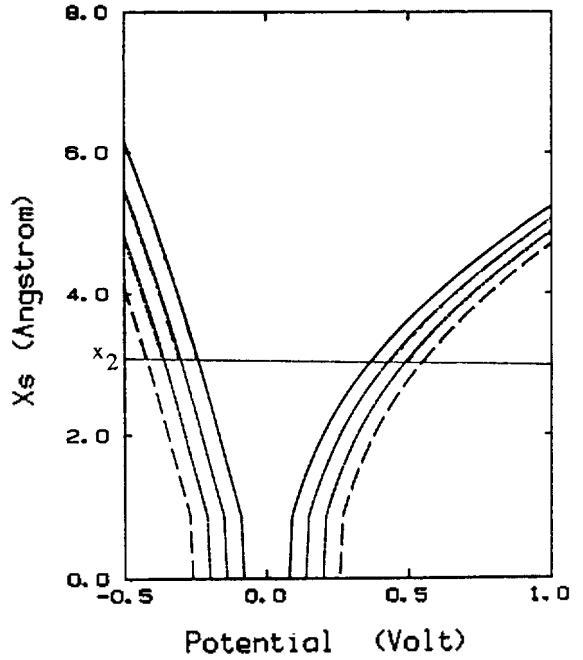


**Figure 11.** The saturation coordinate $x_s$ as a function of potential difference for a few selected electrolyte concenterations. Thick lines indicated the region where $x_s$ is greater than $x_2$.

The potential variation inside the electrode occurs again in an extremely thin surface layer, but is still not negligible (Figure 2 and 3).

About 55%–70% of potential drop occurs at the electrode surface when potential difference between the electrode and bulk liquid is 1.0 V. The effect of the electrode becomes negligible at lower concentration near zero potential (~2% for 0.0001 M around zero potential, in Figure 4). The slope at origin in Figure 3 is closer to one at lower concentration, which also indicates the effect of the electrode is negligible. At higher potential, however, the effect of the electrode becomes significant especially at positive potentials. These are observed in; i) the rapid drop of potential starting at $x$~−0.3 Å in Figure 2, the deviation from a straight line at potential greater than ~0.1 V in Figure 3, ii) the relative potential difference approaching −1 at higher potential indicating a greater portion of potential drop occurs inside the electrode (Figure 4). For a negative potential, the electrode contribution is less important as indicated by; i) the slower increase of potential near $x = 0$ in Figure 2, ii) straighter lines in Figure 3, and iii) closer to zero relative potential differences in Figure 4.

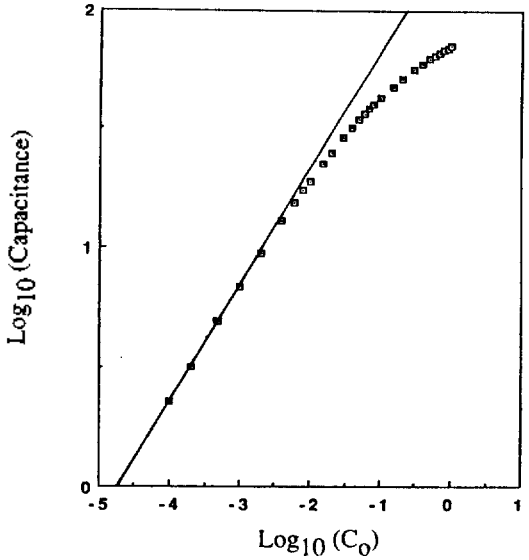


**Figure 12.** Capacitances vs electrolyte bulk concentration graph in a log-log scale at zero potential. The pure effect of size is observed at higher concentrations as the deviation from a straight line.

The apparent asymmetric behavior vs potential reversal are also well interpreted from the asymmetric mechanism in EDL formation. Asymmetries vs potential reversal are observed in ; i) potential profiles inside the electrode (Figure 2), ii) absolute and relative potential drops inside the electrode (Figure 3 and 4), iii) volume and surface charge densities of the electrode (Figure 5 and 6), and iv) capacitances of the EDL (Figure 8). These asymmetries originate from the physical properties of the charge carrier in the electrode. Since there is only one kind of charge carrier in the electrode, that is, electrons with a negligible size ($\leq 10^{-13}$ cm), the distribution function of this charge carrier, electron, is not symmetric with respect to potential reversal. It is relatively harder for electrons to be accumulated than to be deplected and hence the EDL characteristics are also asymmetric.

Comparison of the present results with the prior ones[5] reveals a few point worth mentioning. Observed differences are purely due to the size effect of ion which manifest itself as the constant density regions between the electrode and the electrical diffuse layer. At the outset, the very existence of constant density region inevitably provides a region where some potential drop will occur, and thus this potential drop inside the constant density region will reduce the amount of potential drop both inside the electrode and in the electrical

diffuse layer. This is exactly what is observed as follows; i) potential drop inside the electrode is smaller (55%–70% in Figure 3, compared with 70%–85% of previous results for 1.0 V of potential difference), ii) relative potential drop is closer to zero (Figure 4), iii) the amount of electron depletion or electron accumulation is accordingly reduced (Figure 5), iv) potential drop inside the electrode at negative potential is smaller (Figure 2 and 3), and the final and the most important result is v) a much less abrupt increase of surface charge density (Figure 6) and the consequent disappearing of the diverging increase of the EDL capacitance at negative potential (Figure 8). The previously observed exploding behavior of the EDL capacitances has vanished and they do not diverge even at high concentration (0.1 M) and at high cathodic potential (−0.5 V). Since the measured capacitances at negative potential region are even smaller,[2,13-16] this behavior of the EDL capacitance, especially at negative potential region confirms major improvements accomplished by the present work in describing the real EDL. It can be said that the attempt is at least toward the right direction. On the other hand, the measured EDL capacitances are even smaller and this indicates that there are still rooms for further improvement.

The concentration profiles of the cation (Figure 9) and that of the anion (Figure 10) show the expected behaviors. Both concentrations are zero in the Stern layer, that is, between $x=0$ and $x=x_2$. The counterion concentration, that is, the cation concentration at negative potential and the anion concentration at positive potential decreases extremely rapidly at the very outside of constant density regions and rather slowly in the electrical diffuse layer. The coion concentration, that is, cation concentration at positive potential and anion concentration at negative potential, increases relatively rapidly and it reaches about 85% of bulk concentration at $x=30$°A. When $x_s>x_2$, there is the saturated layer of counterion between $x=x_2$ and $x=x_s$ with its maximum concentration. While the concentration of the counterion is in its maximum, that of the coion is zero in this region. The saturation is observed for the potentials of $\phi_m=0.5$ V and $\phi_m=1.0$ V in Figure 10 and $\phi_m=-0.4$ V in Figure 9. The dependencies of $x_s$ vs applied potential for a few electrolyte bulk concentrations are presented in Figure 11. It is observed that the saturated layer begins to grow starting from potentials higher than 0.3~0.5 V for positive potentials and potential lower than −0.25~−0.4 V for negative potentials (Figure 11).

The behavior of the EDL capacitances according to Gouy-Chapman (GC) theory is well observed at lower concentration, around at zero potential (Figure 8). Electrode effect is minimal at lower concentration around zero potential (Figures. 3, 4 and 6) and capacitance curves have rounded shapes and small values as predicted by GC theory. At higher electrolyte concentration, a graph of the logarithm of capacitance calculated at zero potential vs the logarithm of electrolyte bulk concentration shows the effect of ion size (Figure 12). The slope of the straight line which best fits this capacitance data at lower electrolyte concentrations, is about 0.5 as predicted by GC theory. A deviation from the straight line is observed at electrolyte concentrations higher than ~0.01 M. Since capacitances are calculated at zero potential, that is, since the possible effect due to higher potential is not involved at all into the calculation of these capacitances, this deviation is attributed to the pure size effect of ion, which becomes more significant at higher electrolyte concentration.

As a final remark, since the effects of the ion size is rather well incorporated in the present model, further improvement on the EDL model could be made along the line of electrode/electrolyte boundary wall movement. The boundary could possibly be pushed into the electrolyte at negative potential. Also the specific adsorption of a certain ion to the electrode and the electrostriction, since they would introduce additional charge distribution and consequently lead closer to real potential profiles near the electrode/electrolyte interface, could be well incorporated for a better EDL model.

**Acknowledgement.** The authors gratefully acknowledge the support of this research work by the National Science Foundation through the Grant No. DMR-8812824. One of the authors (SYK) would also like to acknowledge the Research Fellowship Grant from the Johnson Wax Fund, in the early stages of this work.

## Reference

1. (a) G. Gouy, *J. Phys.*, **9**(4), 457 (1910); (b) D. C. Chapman, *Philos. Mag.*, **25**, 475 (1913); (c) O. Stern, *Z. Electrochem.*, **30**, 508 (1924).
2. R. Kofman, R. Garrigos, and P. Cheyssac, *Thin Solid Films*, **82**, 73 (1981).
3. G. A. Martynov and R. R. Salem, *Lecture Notes in Chemistry*, vol. 33, Electrical Double Layer at a Metal-dilute Electrolyte interface, chap. VI, and VII, Springer-Verlag, New York (1983).
4. Wolfgang Schmickler and Douglass Henderson, *J. Chem. Phys.*, **85**(3), 1650 (1986).
5. S. Y. Kim and K. Vedam, *Bull. Korean Chem. Soc.*, **10**, no. 6, 585 (1989).
6. C. Kittel, *Introduction to Solid State Physics*, 5th ed., John Wiley & Sons, Inc., New York (1976).
7. R. Reeves, *Comprehensive Treatise of Electrochemistry*, vol. 1: "The Double Layer", chap. 3, edited by J' O. M. Bockris, B. E. Conway and E. Yeager, Plenum Press, New York and London (1980).
8. J. D. Jackson, *Classical Electrodynamics*, 2nd ed., chap. 4, John Wiley & Sons, Inc., New York (1975).
9. J. A. Dean, *Lande's Handbook of Chemistry*, 12th edition, McGrqaw-Hill Book Company (1978).
10. D. M. Kolb, *J. Vac. Sci. Technol.*, **A4**(3), 1294 (1986).
11. D. M. Kolb and J. Schneider, *Surf. Sci.*, **162**, 764 (1986).
12. M. A. Habib and J. O'M. Bockris, *Comprehensive treatise of Electrochemistry*, vol. 1: "The Double Layer", chap. 4, edited by J. O'M. Bockris, B. E. Conway and E. Yeager, Plenum Press, New York and London (1980).
13. H. A. Latinen and M. S. Chao, *Electrochem. Soc.*, **108** 8, 726(1961).
14. G. M. Schmid and R. N. O'Brien, *J. Electrochem. Soc.*, **11**1, 7, 832 (1964).
15. J. C. Farmer, *J. Electrochem. Soc.*, **132**, (11) 2640 (1985).
16. J. Richer and J. Lipkowski, *J. Electrochem. Soc.*, **133**, 1, 121 (1986)